The effect of nanotube surface oxidation in the electrical response of MWCNT/PVDF nanocomposites

S.A.C. Carabineiro[1], M.F.R. Pereira[1],J. Nunes-Pereira[2], J. Silva[2], C. Caparros[2], V. Sencadas[2,3], S. Lanceros-Méndez[2]

[1] Laboratório de Catálise e Materiais (LCM), Laboratório Associado LSRE/LCM, Faculdade de Engenharia, Universidade do Porto,–, Rua Dr. Roberto Frias, s/n, 4200-465 Porto, Portugal

[2] Centro/Departamento de Física da Universidade do Minho, Campus de Gualtar,4710-057 Braga, Portugal

[3] IPC – Institute for Polymers and Composites, University of Minho, Campus de Azurém, 4800-058 Guimarães, Portugal

Abstract

Carbon nanotubes / poly(vinylidene fluoride) composites were prepared using CNT with different oxidation and thermal treatments. The oxidation procedure leads to CNT with the most acidic characteristics that lower the degree of crystallinity of the polymer and contribute to a large increase of the dielectric constant. The surface treatments, in general, increase percolation threshold and decrease conductivity, but, on the other hand, are able to promote the nucleation of the electroactive phase of the polymer, which is suitable for the use of PVDF in sensors, actuators and other smart materials applications. Finally, the surface treatments do not seem to affect CNT interaction among them, reaching similar degrees of dispersion in all cases, as shown by the SEM results.

The maximum value of the dielectric constant is ~630. It is demonstrated that the composite conductivity can be attributed to a hopping mechanism that is strongly affected by the surface treatment of the CNT.

Keywords: carbon nanotubes, surface functionalization, PVDF composites, electrical properties

Introduction

Carbon allotropes such as single-walled carbon nanotubes (SWCNT) or multi-walled carbon nanotubes (MWCNT) are considered, since the work of Iijima [1], exceptional materials due to their remarkable electrical and mechanical properties [2, 3]. The inclusion of these materials in a polymer matrix improves the mechanical and electrical properties of the polymer [4, 5], and the application range for such material is very broad [6].

Several types of polymers – polypropylene (PP), polycarbonate (PC) and poly(vinylidene fluoride) (PVDF) – have been used to study several physical properties in MWCNT composites. PVDF is the main representative of a family of polymer materials with interesting scientific and technological properties. This polymer is known for its outstanding electroactive properties, non-linear optical susceptibility and high dielectric constant, among polymers [7].

The conductivity of MWCNT/PVDF composites is usually understood within the framework of the percolation theory [8-10]. The percolation theory defines the percolation threshold, a critical concentration at which a giant cluster emerges in the domain marking the beginning of a second order phase transition. Within this theoretical framework, a power law is predicted for the electrical conductivity for concentrations larger than the percolation threshold:

$$\sigma \propto \sigma_0 \left(\Phi - \Phi_c\right)^t \tag{1}$$

where σ is the composite conductivity, σ_0 the filler conductivity,Φ is the filler volume fraction, Φ_c is the critical volume fraction and *t* the critical exponent. It is worth to point that the critical exponents are believed to be universal [11], in contrast with is stated in a recent review [12], that demonstrates the existence of non-universal values for the conductivity critical exponent. It is important to notice that the origin of the conductivity critical exponent is not well understood. On the one hand, there is the Alexander-Orbach conjecture [13] which relates the conductive critical exponent to the system dimension and other critical exponents from the percolation theory, predicting therefore a universal critical exponent. On the other hand, several models have been proposed for the origin of a non-universal conductivity critical exponent,

[14]. Using hopping between the fillers as conduction model [15], it results in a conduction critical exponent that is equal to that predicted by the effective medium theory [16].

One of the first attempts to include CNT in a PVDF matrix was performed in 2003 by Seoul *et. al* [17]. The production of SWCNT/PVDF composites and the composite conductivity in the solution was reported for spin-coated films and electrospun fiber mats. A percolation threshold for the conductivity of 0.003 wt % was found for SWCNT/PVDF solutions, 0.015 wt % for SWCNT/PVDF spin-coated films and 0.04 wt % for SWCNT/PVDF electrospun fiber mats. The dielectric properties of MWCNT/PVDF composites prepared by a physical blending and hot-moulding process [18] increases rapidly with increasing CNT volume fraction, leading for values of the dielectric constant as high as 300 with a percolation threshold of 1.61 %vol. The conduction mechanism is described by the formation of a conductive network through hopping and tunneling processes. MWCNT/PVDF composites were also prepared by a solution method and hot moulding technology [19].The effect of stretching in the electrical properties of the nanocomposites was studied, demonstrating that the dielectric constant and conductivity decrease with stretching, due to the rearrangement of MWCNT in the composites along the tensile-strain direction. The effects of varying MWCNT aspect ratio in MWCNT/PVDF composites [20] was also studied, with an increase of the dielectric constant with increasing MWCNT aspect ratio. Further, the percolation threshold increases with increasing aspect ratio, in contrast with the accepted $\propto 1/L$ scaling for the percolation threshold, where L is the length of the filler [21, 22]. This fact was attributed to the MWCNT agglomeration that reduces the effective aspect ratio. Finally, it was demonstrated that the dielectric constant follows a power law that is in accordance to the percolation theory [8-10], with a critical exponent that depends on the MWCNT aspect ratio, i.e. non-universal critical exponent MWCNT/PVDF composites prepared by a melt-compounding approach [23] show percolation threshold between 2 and 2.5 wt% for the composites conductivity. It has been also reported that the inclusion of MWCNT in a PVDF matrix acts as a nucleation agent producing the polar β PVDF crystal form [24]. Furthermore, by mixing MWCNT with PVDF in the molten state in an ultra high-shear extruder[25], it was demonstrated that the percolation threshold depends on the shear, being 2.5 wt% for samples obtained under low-shear processing

and 1.5 wt% for samples obtained under high-shear processing. In MWCNT/PVDF samples produced by solution casting [26], a percolation threshold of 0.23 vol% (0.19 wt%) was reported for the conductivity, whereas no percolation threshold was found relative to the dielectric constant. Instead, it was possible to infer that between 0.12 vol% and 0.23 vol% there is a jump in the dielectric constant, less than one order of magnitude, at 1 kHz. Electrospun SWCNT/PVDF and MWCNT/PVDF composites with the fillers having similar surface chemistry were also studied [27]. The focus was in the crystalinity and in interfacial interaction between filler-matrix of the electrospun nanofibers. A decrease in the electrical conductivity with increasing filler concentration was observed. In particular, when the concentration of MWCNT and SWCNT was increased from 0.01 wt% to 0.1 wt%, the electrical conductivity was reduced, in contrast to previous results. In this context, it was demonstrated that the formation of a capacitor network for MWCNT/PVDF composites is the main mechanism for the enhancement of the dielectric constant, and it is also responsible for the deviations from the percolation theory [28, 29]. Furthermore, it was shown that the PVDF degree of crystallinity also influences the electrical properties of the composite [30].

In this type of composites, the main problem is controlling the filler dispersion and the matrix-filler interaction. Attempts have been made by preparing spherical composite particles by sonication [31] and different mixing procedures [32], but some of the most interesting strategies include the functionalization of the fillers. In 2007, Dang *et. al* [33] presented a wet-chemistry procedure to prepare functionalized MWCNT/PVDF composites. The MWCNT were modified with 3,4,5 trifluorobromobenzene (TFBB) in order to improve their dispersion in PVDF. A value of 8000 for the dielectric constant was reported, although with a large dielectric loss. The percolation threshold was investigated by fitting a power law to the experimental results, observing a percolation threshold of 8 vol % and non-universal critical indices. It is important to note that by functionalizing the MWCNT, the dielectric constant increases relatively to the pristine MWCNT, due to blocking of the charge carriers by the functional groups. In 2008, a procedure to functionalize the MWCNT was presented by Li *et. al* [34]. Pristine, carboxylic and ester functionalized MWCNT were used to produce MWCNT/PVDF composites by evaporating suspensions of the nanotubes in PVDF. A percolation threshold was reported around 3.8 vol% for the three types of MWCNT/PVDF composites and it was found that for the same

MWCNT concentration, 6 vol%, the conductivity of the pristine MWCNT/PVDF composite is nearly two orders of magnitude larger than that of the functionalized MWCNT/PVDF composite. This fact was explained by a reduction of the MWCNT length, due to the use of the functional groups. A linear relation, $\log(\sigma) \propto \Phi^{-1/3}$ between the conductivity and the volume fraction was also found, that is typical of fluctuation-induced tunnelling [35], but also for hopping between adjacent fillers, corresponding to a weak disorder regime [36]. The electrical properties of pristine MWCNT/PVDF and functionalized (oxidized) MWCNT/PVDF composites have been also studied [37-39]. It was found that the interfacial polarization is the main reason for the enhancement of the dielectric constant with the addition of MWCNT, which is higher for the functionalized MWCNT. It was also reported that the percolation threshold is ~ 3.8 vol% for the electrical conductivity and that the conductivity of the pristine MWCNT is higher than that of the functionalized material for the same vol%, due to a reduction of the MWCNT length, caused not only by the oxidization procedure but also by differences in the aggregation of the fillers.

In the above description, it is evident that the mechanism of conductivity itself and the role of filler surface characteristics in the overall electrical result is not stated. In order to systematically address these issues, this work describes the effect of MWCNT surface functionalization through oxidation and selective removal of oxygen-containing surface groups at different temperatures on the phase content, degree of crystallinity and morphology of the samples. Moreover, the electrical response is studied and its origin is theoretically investigated.

Experimental

Commercial multi-walled carbon nanotubes (Nanocyl - 3100) have been used as received (sample CNTs). Further details on this material can be found elsewhere [40]. CNTs sample was functionalised as described in an earlier work [41]. Briefly, oxidation under reflux with HNO_3 (7 M) for 3 h at 130 ºC was carried out, followed by washing with distilled water until neutral pH, and drying overnight at 120 ºC (sample CNTox). The CNTox material was heat treated under inert atmosphere (N_2) at 400 ºC for 1 h (sample CNTox400) and at 900 ºC for 1h (sample CNTox900), in order to selectively remove surface groups. The obtained samples were characterised

by adsorption of N_2 at -196 ºC, temperature programmed desorption (TPD). The total amounts of CO and CO_2 evolved from the samples were obtained by integration of the TPD spectra.

Polymer films with thicknesses between 100 and 150 μm were produced by mixing different amounts of MWCNT (0.1, 0.15, 0.2, 0.25, 0.5 and 1.0 wt%, corresponding to 1.17×10^{-3}, 1.76×10^{-3}, 2.34×10^{-3}, 2.92×10^{-3}, 5.83×10^{-3} and 1.16×10^{-2} volume fractions – Φ) with N,N dimethylformamide (DMF, Merck 99.5%) and PVDF (Solef1010, supplied by Solvay Inc., molecular weight = 352×103 g/mol) according to the procedure previously described [42]. For the calculation of the volume fraction the same density has been considered for all MWCNT independently of the oxidation treatment. Solvent evaporation, and consequent crystallization, was performed inside an oven at controlled temperature. The samples were crystallized for 60 min at 120 °C to ensure the evaporation of all DMF solvents. After the crystallization process, the samples were heated until 230 °C and maintained at that temperature for 15 min to melt and erase all polymer memory. This procedure should produce α-PVDF crystalline phase samples [43].

The crystalline phase or phases present in the composites were identified by Fourier transform infrared spectroscopy (FTIR) using a Perkin-Elmer Spectrum 100 apparatus in ATR mode from 4000 to 650 cm^{-1}. FTIR spectra were collected after 32 scans with a resolution of 4 cm^{-1}.

The thermal behavior of the samples was evaluated by differential scanning calorimetry (DSC), using a Pyris apparatus from Perkin-Elmer. Samples of MWCNT/PVDF were cut into small pieces and placed in aluminium cans with perforated lids and heated from 30 to 200 ºC, at a heating rate of 10ºC/min, in order to estimate the melting temperature and the degree of crystallinity of each sample.

The topography of the samples and the MWCNT distribution was analysed by scanning electron microscopy (SEM, FEI – NOVA NanoSEM 200).

The dielectric response of the nanocomposites was evaluated by dielectric measurements with a Quadtech 1920. The real (ε') and imaginary part of the permittivity (ε'') were obtained in the frequency range of 500 Hz to 1 MHz at room temperature. The d.c. electrical volume conductivity of the samples was obtained by measuring the characteristic I-V curves at room temperature with a Keithley 6487 picoammeter/voltage source. The current and voltage were measured and the

resistivity was calculated taken into account the geometrical factors. For the dielectric and the d.c. electrical measurements, circular gold electrodes of 5 mm diameter were previously evaporated by sputtering onto both sides of each samples.

Results

The oxidising treatment originates materials with large amounts of surface acidic groups, mainly carboxylic acids and, to a smaller extent, lactones, anhydrides and phenol groups [40, 41, 44, 45], formed at the edges/ends and defects of graphitic sheets [46]. The different surface oxygenated groups decompose by heating, releasing CO and/or CO_2, during a thermal programmed desorption (TPD) experiment. As this release occurs at specific temperatures, identification of the surface groups is possible [40, 41, 44, 45].

Table 1 - BET surface areas obtained by adsorption of N_2 at -196ºC and amounts of CO_2 and CO obtained by integration of areas under TPD spectra (adapted from [41]).

Sample	S_{BET} (m^2/g)	pH_{PZC}	CO_2 (μmol/g)	CO (μmol/g)	CO / CO_2
CNTs	254	7.3	70	193	2.76
CNTox	400	4.2	778	1638	2.11
CNTox400	432	6.9	230	1512	6.57
CNTox900	449	7.4	24	204	8.50

The total amounts of CO and CO_2 evolved from the samples, obtained by integration of the TPD spectra, are presented in Table 1. It is clear that the treatment with HNO_3 produces a large amount of acidic oxygen groups, which decompose to release CO_2. Part of these groups (carboxylic acids) are removed by heating at 400 ºC. A treatment at 900 ºC removes almost all the groups, so that the obtained surface chemistry is similar to that of the original sample.. The CNTox sample has the highest amount of surface oxygen. This sample also presents the lowest ratio CO/CO_2, indicating that this is the most acidic sample. CNTox900 presents the highest CO/CO_2 ratio, suggesting the less acidic characteristics. The acid character of the samples decreases by increasing the thermal treatment temperature, since the acid groups are removed at lower temperatures than neutral and basic groups, as seen in previous works [40, 41, 44, 45], and in agreement with the pH_{PZC} values of the samples.

The surface areas of the samples, calculated by the BET method (S_{BET}), are included in Table 1. The oxidation treatments lead to an increase of the surface area, as the process opens the endcaps of CNTs and creates sidewall openings [47]. The surface areas slightly increase as the thermal treatment temperature increases, since carboxylic acids and other groups, introduced during oxidation, are removed.

FTIR was used to identify the phase or phases present in the samples. The presence of α-PVDF can be identified by the 766 cm^{-1} absorption band and the presence of the β-phase by the 840 cm^{-1} absorption band [48-50]. Fig. 1 shows the FTIR spectra for the four functionalized MWCNTs at 2.92×10^{-3} volume fraction (Φ) and for the MWCNT/PVDF samples at all volume fractions.

The characteristic absorption bands for the α- and β–PVDF are present in all samples, apart from the pure polymer without MWCNT fillers, which is fully in the α phase PVDF, after processing under the same conditions as the composite samples. From the FTIR curves, the amount of α (F_α) and β-phase (F_β) can be calculated by equation 2, following the procedure described elsewhere [43, 51].

$$F(\alpha) = \frac{A_\alpha}{(K_\alpha / K_\beta)A_\beta + A_\alpha} \qquad (2)$$

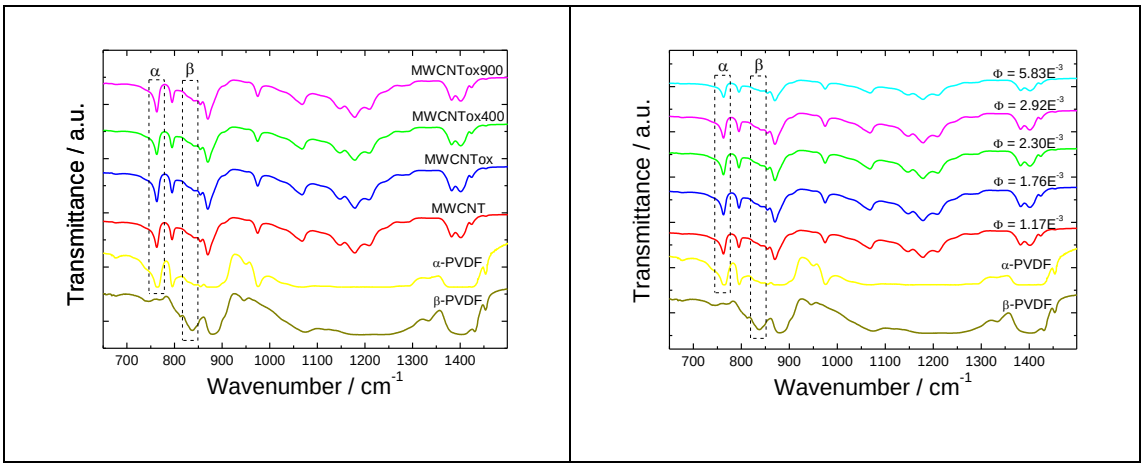

Figure 1. Left: FTIR spectra of the different functionalized MWCNTs polymer composites at 2.92×10^{-3} Φ; Right: FTIR spectra obtained for the PVDF/MWCNT composites at different volume fractions.

In equation 2, F(α) represents the α-phase content; A_α and A_β the absorbencies at 766 and 840 cm^{-1}, corresponding to the α and β-phase material, respectively; K_α and K_β

are the absorption coefficient at the respective wave number. The values of K_α and K_β are 7.7×10^4 and 6.1×10^4 cm^2/mol, respectively [43, 51].

Figure 2 shows the quantification of α and β-phase for composites at $\Phi = 2.92\times10^{-3}$ for the different functionalized MWCNTs/PVDF samples and as a function of volume fraction for the MWCNT/PVDF composites.

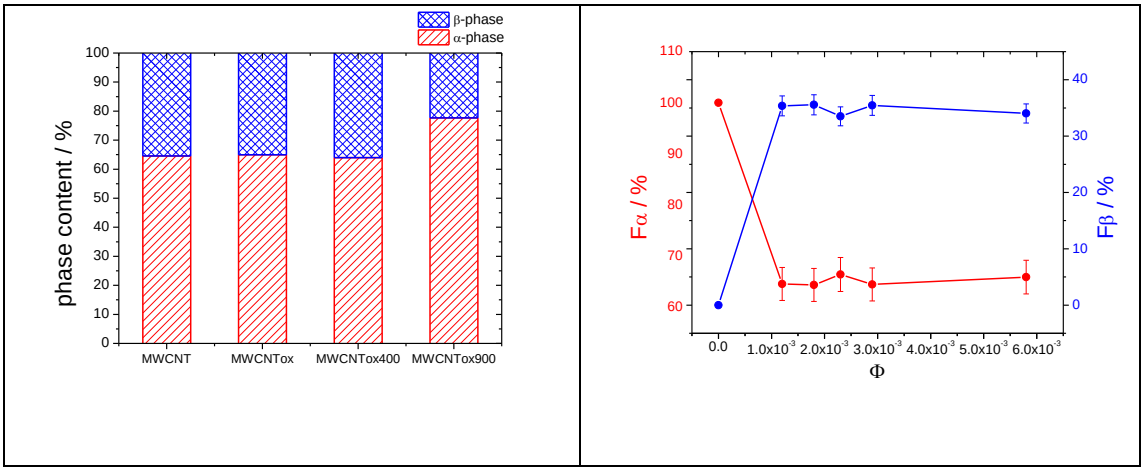

Figure 2. α (F_α) and β-phase (F_β) content for (left) the four functionalized MWCNT/PVDF composites at $\Phi = 2.92\times10^{-3}$ and (right) as a function of volume fraction for MWCNT/PVDF composites.

Figure 2 shows that all samples present a mixture of α and β-PVDF phases, with the α-phase content of the polymer ranging from 64.0% to 77.7%. The larger value of α-phase was obtained for CNTox900 composite, corresponding to the less acidic sample and with a larger surface area. In any case, it can be concluded that the surface treatments does not have strong influence in the nucleation of the electroactive β phase of the polymer.

DSC thermographs were used to determine the melting characteristics and to calculate the degree of crystallinity of the composites. The DSC curves for the four functionalized MWCNT at $\Phi = 2.92\times10^{-3}$ and for MWCNT/PVDF composites at different volume fractions are presented in Figure 3.

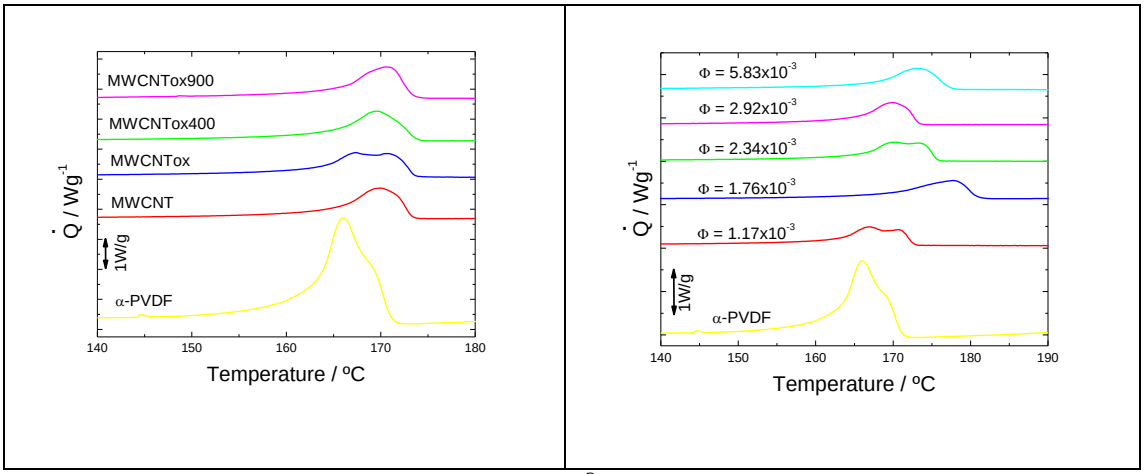

Figure 3. DSC scans obtained for 2.92×10^{-3} Φ of the different functionalized CNTs (left) and scans obtained for the MWCNT/PVDF composites at different volume fractions (right).

In Figure 3 (left) it is shown that the melting temperature of the composites is shifted to higher temperature with respect to α-PVDF, due to the presence of the β-phase of the polymer with a higher thermal stability. In Figure 3 (right) it is shown that the shift to higher temperatures occurs for all concentrations above $1.17\text{x}10^{-3}$ which is correlated to the fact that all composite samples show a similar phase content.

The degree of crystallinity (χ_c) was calculated (Eq. 3) from the enthalpy of the melting peak (ΔH_f) of the DSC scans, taken into consideration the enthalpy of a fully crystallized PVDF ($\Delta H_{100\text{-}\alpha} = 93.07$ Jg^{-1}; $\Delta H_{100\text{-}\beta} = 103.4$ Jg^{-1}) and the relative fraction of α (x) and β-phases (y)[7].

$$\chi_c = \frac{\Delta H_f}{x\Delta H_{100-\alpha} + y\Delta H_{100-\beta}} \times 100 \qquad (3)$$

In Figure 4 the degree of crystallinity is shown for composites with 2.92×10^{-3} MWCNT volume fraction and for the MWCNT/PVDF composites at different volume fractions.

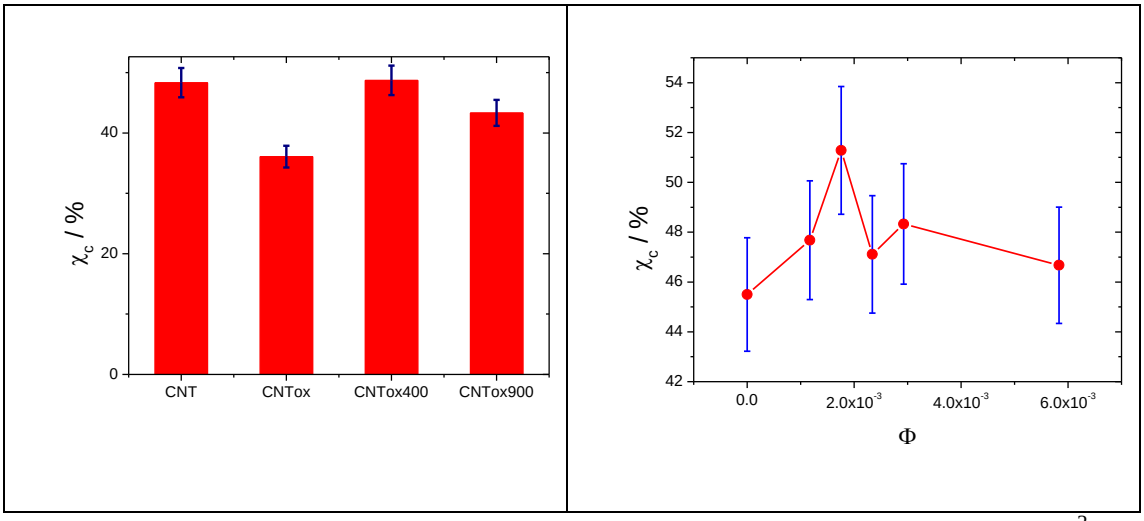

Figure 4. Degree of crystallinity (χ_c) of the four types of MWCNT at 2.92×10^{-3} Φ (left) and as a function of volume fraction for MWCNT/PVDF composites (right).

Figure 4 indicates that there are not large variations of the degree of crystallinity, neither with the surface treatment of the CNT, nor with the variation in concentration for a given type of CNT. The degree of crystallinity is nevertheless smaller for the more acidic sample (CNTox), indicating larger surface interaction and hindering perfect crystallisation of the polymer.

The morphology and fiber distribution of the prepared samples were analyzed by SEM. Fig. 5 shows representative images of the prepared samples.

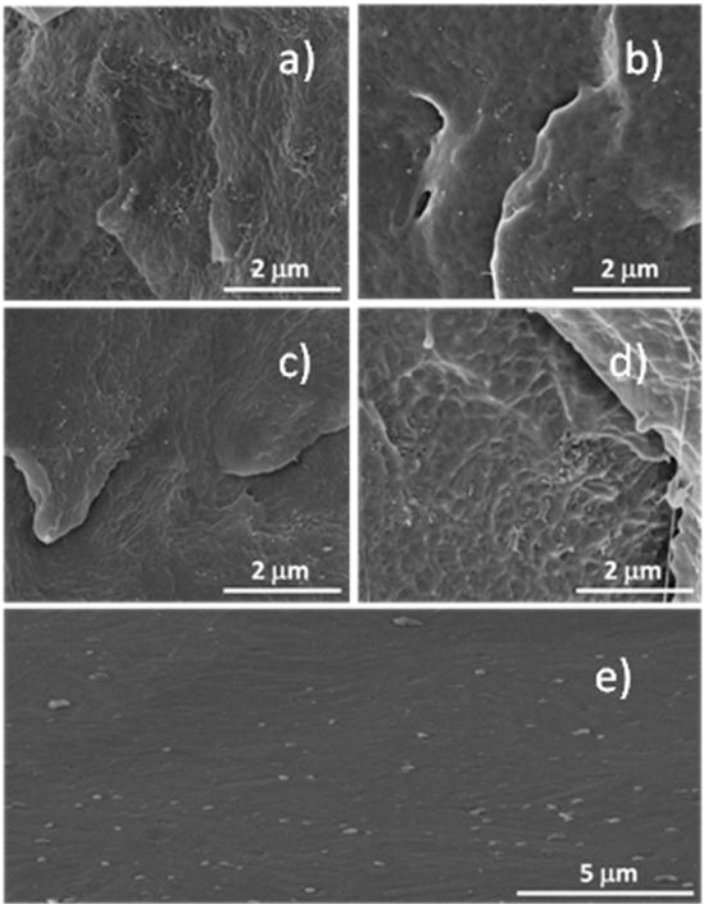

Figure 5. SEM images of composites at 2.34×10^{-3} Φ: a) fracture image of a MWCNT/PVDF sample; b) fracture image of a MWCNTox/PVDF sample; c) fracture image of a MWCNTox400/PVDF sample; d) fracture image of a CNTox900/PVDF sample; e) surface image of a MWCNTox900/PVDF.

The fracture images (Figure 5 a) to d)) demonstrate that there is a good dispersion of the MWCNT in the polymer matrix and that the degree of dispersion is similar for the different functionalized MWCNT samples. The surface images (Figure 5 e)) demonstrate that the spherulitic structure characteristic of pure α-PVDF is still present in the composite samples, indicating that the fillers, independently of their surface treatment, do not have a strong influence in the crystallization dynamics.

Electrical measurements were performed to investigate the influence of the different CNT surface treatments in the overall electrical response of the composites. Dielectric constant and AC conductivity were measured for all MWCNT/PVDF composites.

Figure 6 shows the dielectric constant as a function of the frequency for the (MWCNTox) MWCNT/PVDF composites.

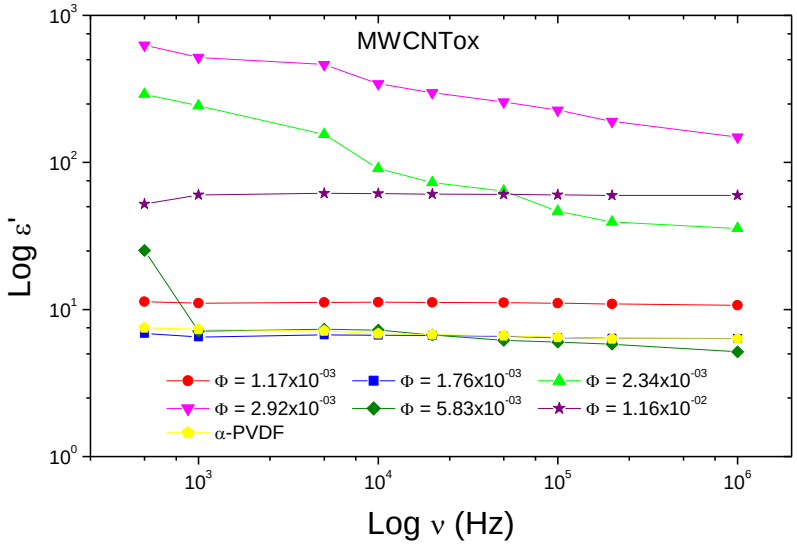

Figure 6. Dielectric constant (ε') as a function of frequency (ν) for the (CNTox) MWCNT/PVDF composites.

Figure 6 shows that the dielectric constant for the (CNTox) MWCNT/PVDF composites is almost independent of the frequency, except for the volume fractions 2.34×10^{-3} and 2.92×10^{-3}An increase in the dielectric constant is notorious, when compared with the α-PVDF, for the samples with 2.34×10^{-3}, 2.92×10^{-3} and 1.16×10^{-2} Φ of MWCNT.

The frequency dependent dielectric constant, obtained for the MWCNTs composite samples, prepared with the different CNT treatments, show similar trends as those seen in Fig. 6.

Fig. 7 shows the electrical conductivity as a function of frequency for MWCNTox/PVDF samples for the different volume fractions studied, calculated by equation 4 [52]:

$$\sigma = \omega\varepsilon_0\varepsilon'' \qquad (4)$$

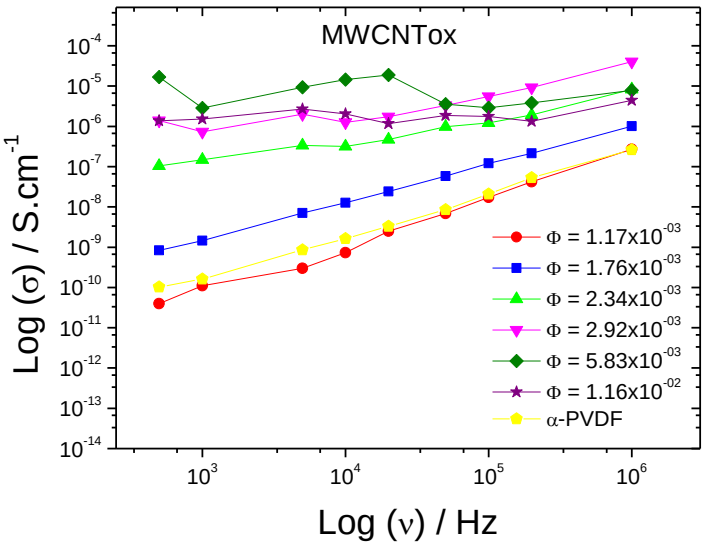

Figure 7. Conductivity (σ) for the MWCNTox composites as a function of frequency (ν).

As a general trend, the electrical conductivity increases with increasing frequency for the MWCNTox /PVDF samples. This increase is observed for all samples with the exceptions of the composites with higher filler volume fraction ($5.83x10^{-3}$ and $1.16x10^{-2}$), which show a frequency independent behaviour. Moreover, the conductivity of the composites increases with increasing volume fraction of MWCNT. These trends are observed also for the composites with CNT undergoing different surface treatments. The fact that the samples with higher volume fractions show a frequency independent conductivity, leads to conclude that the increase in the conductivity with frequency for some of the samples is intrinsic to the matrix and it is related to ionic conductivity of the PVDF matrix.

Figure 8 shows the dielectric constant as a function of volume fraction for the four types of MWCNT composites at a frequency of 1 kHz at room temperature.

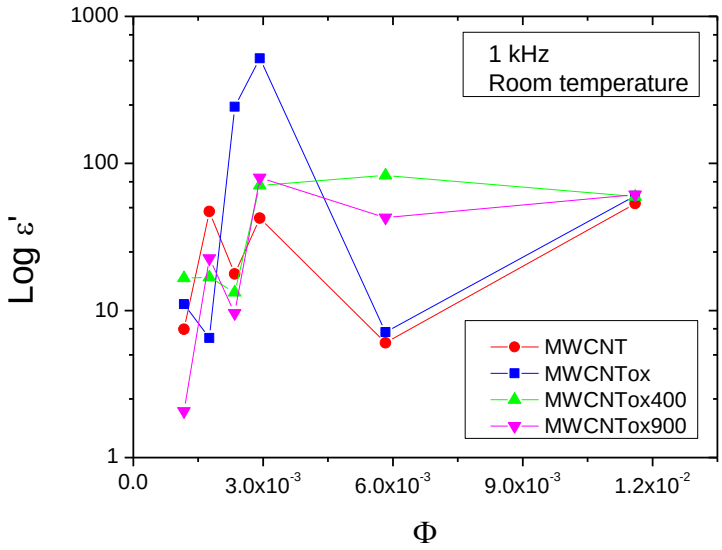

Figure 8. Dielectric constant (ε') as a function of volume fraction (Φ) for the different surface treatments performed on MWCNTs samples.

The larger values of the dielectric constant are obtained for the oxidised CNT with a volume fraction of 2.92×10^{-3} (0.25 wt%); the obtained value of ~ 630 is in accordance to the recent literature. It is worth to notice that the larger values of the dielectric constant are obtained for the more acidic sample. The higher value of the dielectric constant is achieved for lower volume fractions (two orders of magnitude) than Dang *et. al* [33] (0.15) but with lower values of the dielectric constant than these authors. Comparing with Li *et. al* [34], the higher value of the dielectric constant is also achieved for a lower volume fraction. As a function of concentration, Figure 8 shows an increase of the dielectric constant with volume fraction, followed by a decrease. This behaviour is typical of this type of composites and can be explained by the percolation theory.

Figure 9 shows the concentration dependence of the DC conductivity for the different composites (left) obtained from the characteristic I-V curves (right).

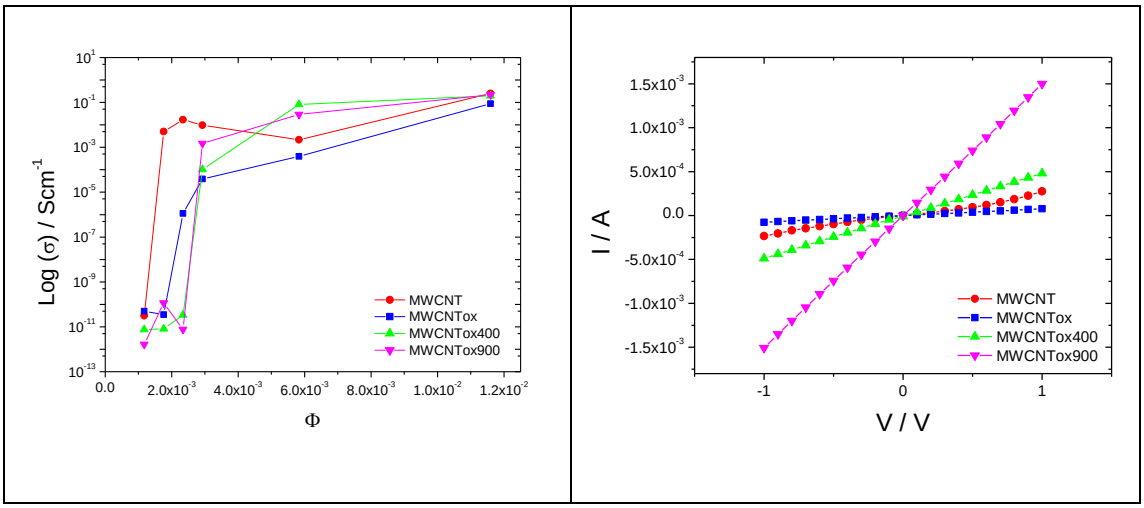

Figure 9. DC conductivity (σ) as a function of volume fraction (Φ) for the different functionalized MWCNTs (left), and characteristic IV curves for the different functionalized MWCNTs at 5.83×10^{-3} Φ (right).

It can be observed that the pristine MWCNT have a lower percolation threshold than the functionalized ones, which is in contrast to the same percolation threshold for the pristine and functionalized MWCNT obtained in the literature [34, 37]. The latter authors explain the higher conductivity obtained for composites with pristine MWCNT with a reduction of the length of the MWCNT. It is important to notice that if there is a reduction in the length of the MWCNT, different percolation threshold should be observed, which is not the case of the latter works.

As the conductance of the MWCNT is mainly determined by the π orbital's [2], when the MWCNT are surface treated or functionalized, and the functional groups or defects are related to π orbitals, the conductance of the MWCNT is lowered and therefore the functionalized composites should show, in general, lower conductivity.

Discussion

It is important to notice that the oxidation procedure leads to samples with higher acidity, which induces a reduction of the degree of crystallinity of the polymer and an enlargement of the dielectric constant and lowering of the conductivity for a given concentration in the composite, due to the inclusion of defects in the surface of the

CNT. The surface treatments in general increase percolation threshold and decrease conductivity, but, on the other hand, are able to promote the nucleation of the electroactive phase of the polymer, which is suitable for the application of PVDF in sensors, actuators and other smart materials applications. The nucleation of the electroactive phase of the polymer is related to electrostatic interactions between the surface treated CNT and the polar groups of PVDF [48]. Finally, the surface treatments do not seem to affect CNT interaction among them, reaching similar degrees of dispersion in all cases, as shown by the SEM results.

A more quantitative assessment of the electrical properties was achieved by analysing the results from Figure 9 with equation (1) from the percolation theory, but the obtained results are inconclusive, indicating that the theory is not appropriate for the proper description of the observed behaviour. Then, a description based on the network theory was applied, that allows to relate the composite conductance to the network disorder, by mapping the fillers to the vertices of the network and the edges to the gaps between the fillers [36]:

$$G_{eff} = G_{cut} \exp\left(\frac{-l_{opt}}{(N_{\max}\Phi)^{\frac{1}{3}}}\right) \quad (5)$$

In this equation, l_{opt} is the length of the optimal path, that is the single path for which the sum of the weights along the path is the minimum. When most of the links of the path contribute to the sum, the system is said to be in the ”weak disorder” regime [53]. Conversely, the situation where a single link dominates the sum along the path is called the strong disorder limit [53]. In Equation (5), N_{max} is the maximum number of fillers in the domain and G_{cut} is the effective conductance of the system before a bond with maximum conductance is added to (or removed from) the system [53]. The l_{opt} parameter is related to the disorder strength when the system is in the weak disorder regime. At the weak disorder regime, the disorder strength is just the inverse of the scale over which the wave function decays in the polymer (x_0), as expressed by the hopping conductivity equation at room temperature [35, 54].

$$\sigma_{ij} = \sigma_0 \exp\left(-\frac{x_{ij}}{x_0}\right) \quad (6)$$

In Equation (6), σ_0 is the dimension coefficient and x_{ij} is the distance between two fillers. As described in [36], applying Equation (6) to the gap between the fillers (described as the minimum distance between two rods) and defining the conductivity by hopping between adjacent fillers, results in Equation (5). This gives rise to the expression $\log(\sigma) \propto \Phi^{-\frac{1}{3}}$, as given by Equation (5), which corresponds to a weak disorder regime. This relation is also found in fluctuation-induction tunnelling [35] for the d.c. conductivity. In order to prove the latter assumptions, the $\log(\sigma) \propto \Phi^{-\frac{1}{3}}$ dependence was tested for the d.c. measurements. Figure 10 shows the logarithmic plot of the d.c. conductivity as a function of volume fraction for all MWCNT/PVDF composite samples.

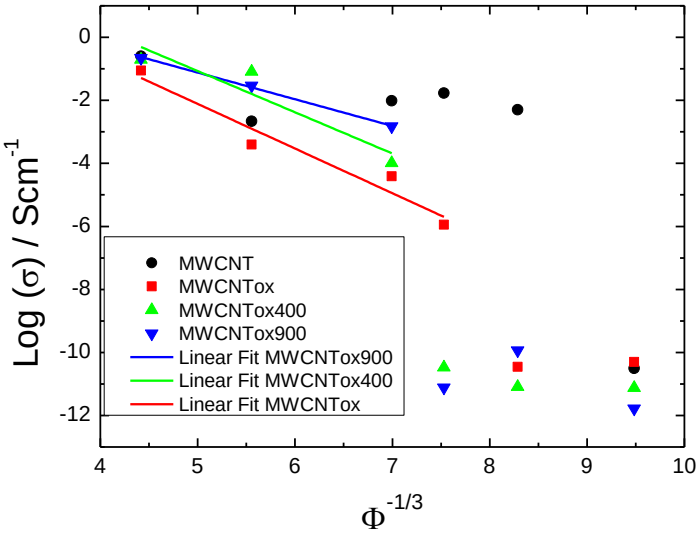

Figure 10. Logarithmic plot of the d.c. conductivity (σ) as a function of volume fraction (Φ) for the different composites. Thick lines are linear fits to the presented data, $R^2 \sim 0.9$

As can be observed in Figure 10, there is a linear relation between the logarithm of the conductivity, but only for the higher volume fractions. A deviation from this behaviour was observed for the lower volume fractions and for the composites prepared with pristine MWCNT. This indicates that the composite conductivity is in the weak disorder regime [36] as the $\log(\sigma) \propto \Phi^{-\frac{1}{3}}$ dependence is observed. The deviation from the linear relation can be described by Equation (5), when the conductive network is not yet formed, which implies that $G_{eff} = G_{cutt}$ [36], i.e., the effective conductance is controlled by the matrix conductance. This fact indicates that

the network is only formed by capacitors at the lower volume fractions and the matrix dominates the overall conductivity. As a conclusion, hopping between nearest fillers explains the deviation from the percolation theory and the overall composite conductivity is explained by the existence of a weak disorder regime. The formation of a capacitor network [29], where the plates of each capacitor are MWCNT pairs, explains the deviation from the expected linear relation between the logarithm of the conductivity and volume fraction, as predicted by the weak disorder regime. On the hand, the fact that the linear relation is not present in the composites prepared with pristine MWCNT indicates that the surface treatment of the CNT determines the nature of the transition of the isolator to the conductive regime, as well as the conduction mechanism of the composites.

Conclusions

Carbon nanotubes / poly(vinylidene fluoride) composites were prepared with different oxidation and thermal treatments. It is demonstrated that functionalized MWCNT can be used to increase the dielectric constant at very low volume fractions. It is also demonstrated that the composite conductivity can be attributed to a hopping mechanism. The oxidation procedure leads to CNT with the most acidic characteristics. These CNT lead to samples with lower degree of crystallinity of polymers and contribute to a large increase of the dielectric constant. The surface treatments lead to CNT that increase percolation threshold and decrease conductivity, but with the ability to promote the nucleation of the electroactive phase of the polymer, which is suitable for the use of PVDF in smart materials applications.

Acknowledgements

The authors thank the Fundação para a Ciência e a Tecnologia (FCT), Portugal, for financial support through the projects PTDC/CTM/69316/2006 and NANO/NMed-SD/0156/2007), and CIENCIA 2007 program for S.A.C.; V.S., J.S. and J.N.P. also thank FCT for the SFRH/BPD/63148/2009, SFRH/BD/60623/2009 and SFRH/BD/66930/2009 grants.

References

1. Iijima, S., *Helical microtubles of graphitic carbon.* Nature, 1991. **354**: p. 56-56.
2. Charlier, J.-C., X. Blase, and S. Roche, *Electronic and transport properties of nanotubes.* Reviews of Modern Physics, 2007. **79**(2): p. 677-732.
3. Thostenson, E.T., C. Li, and T.-W. Chou, *Nanocomposites in context.* Composites Science and Technology, 2005. **65**(3-4): p. 491-516.
4. Moniruzzaman, M. and K.I. Winey, *Polymer Nanocomposites Containing Carbon Nanotubes.* Macromolecules, 2006. **39**(16): p. 5194-5205.
5. L.P.Biró, C.A.B., G.G.Tibbets and Ph. Lambin, *Carbon Filamets and Nanotubes: Common Origins, Differing Applications?* NATO Science Series, ed. S.E.A. Sciences. 2001, Dordrecht: Kluwer Academic Plublishers.
6. Baughman, R.H., A.A. Zakhidov, and W.A. de Heer, *Carbon Nanotubes--the Route Toward Applications.* Science, 2002. **297**(5582): p. 787-792.
7. Lovinger, A.J., *Developments in Crystalline Polymers*, ed. D.C. Bassett. 1982, London: Elsevier Applied Science.
8. Stauffer, D. and A. Aharony, *Introduction to Percolation Theory*. 1992, London: Taylor and Francis.
9. Essam, J.W., *Percolation theory.* Reports on Progress in Physics, 1980. **43**: p. 53-53.
10. Nan, C.W., Y. Shen, and J. Ma, *Physical Properties of Composites Near Percolation.* Annual Review of Materials Research. **40**(1): p. 131-151.
11. Griffiths, R.B., *Dependence of critical indices on a parameter.* Physical Review Letters, 1970. **24**(26): p. 1479-1482.
12. Bauhofer, W. and J.Z. Kovacs, *A review and analysis of electrical percolation in carbon nanotube polymer composites.* Composites Science and Technology. **In Press, Corrected Proof**.
13. Alexander, S. and R. Orbach, *Density of states on fractals : « fractons ».* J. Physique Lett., 1982. **43**(17): p. 625-631.
14. Vionnet-Menot, S., et al., *Tunneling-percolation origin of nonuniversality: Theory and experiments.* Physical Review B, 2005. **71**(6): p. 64201-64201.
15. Silva, J., et al., *The influence of matrix mediated hopping conductivity, filler concentration, aspect ratio and orientation on the electrical response of carbon nanotube/polymer nanocomposites.* Composites Science and Technology, 2011. **71**: p. 643-646.
16. Kirkpatrick, S., *Percolation and Conduction.* Reviews of Modern Physics, 1973. **45**(4): p. 574.
17. Chang Seoul, Y.-T.K., Chi-Kyung Baek,, *Electrospinning of poly(vinylidene fluoride)/dimethylformamide solutions with carbon nanotubes.* Journal of Polymer Science Part B: Polymer Physics, 2003. **41**(13): p. 1572-1577.
18. Wang, L. and Z.-M. Dang, *Carbon nanotube composites with high dielectric constant at low percolation threshold.* Applied Physics Letters, 2005. **87**(4): p. 042903-3.
19. Dang, Z.M., S.H. Yao, and H.P. Xu, *Effect of tensile strain on morphology and dielectric property in nanotube/polymer nanocomposites.* Applied Physics Letters, 2007. **90**(1).
20. Yao, S.-H., et al., *Influence of aspect ratio of carbon nanotube on percolation threshold in ferroelectric polymer nanocomposite.* Applied Physics Letters,

2007. **91**(21): p. 212901-3.
21. Balberg, I., et al., *Excluded volume and its relation to the onset of percolation.* Physical Review B, 1984. **30**(7): p. 3933.
22. Bug, A.L.R., S.A. Safran, and I. Webman, *Continuum Percolation of Rods.* Physical Review Letters, 1985. **54**(13): p. 1412.
23. Hong, S.M., et al., *Physical properties of multi-walled carbon nanotube-filled PVDF composites prepared by melt compounding.* Molecular Crystals and Liquid Crystals, 2007. **464**: p. 777-785.
24. Kim, G.H. and S.M. Hong, *Structures and Physical Properties of Carbon Nanotube Reinforced PVDF Composites.* Molecular Crystals and Liquid Crystals, 2007. **472**: p. 161 - 169.
25. Chen, G.X., Y.J. Li, and H. Shimizu, *Ultrahigh-shear processing for the preparation of polymer/carbon nanotube composites.* Carbon, 2007. **45**: p. 2334-2340.
26. Almasri, A., et al., *Characterization of solution-processed double-walled carbon nanotube/poly(vinylidene fluoride) nanocomposites.* Macromolecular Materials and Engineering, 2008. **293**(2): p. 123-131.
27. Huang, S., et al., *Electrospinning of Polyvinylidene Difluoride with Carbon Nanotubes: Synergistic Effects of Extensional Force and Interfacial Interaction on Crystalline Structures.* Langmuir, 2008. **24**(23): p. 13621-13626.
28. Simoes, R., et al., *Influence of fiber aspect ratio and orientation on the dielectric properties of polymer-based nanocomposites.* Journal of Materials Science, 2009. **45**: p. 268-270.
29. Simoes, R., et al., *Low percolation transitions in carbon nanotube networks dispersed in a polymer matrix: dielectric properties, simulations and experiments.* Nanotechnology, 2009. **20**: p. 35703.
30. Costa, P., et al., *The effect of fibre concentration on the [alpha] to [beta]-phase transformation, degree of crystallinity and electrical properties of vapour grown carbon nanofibre/poly(vinylidene fluoride) composites.* Carbon, 2009. **47**: p. 2590-2599.
31. Zhao, Z.D., et al., *Electrical conductivity of poly(vinylidene fluoride)/carbon nanotube composites with a spherical substructure.* Carbon, 2009. **47**(8): p. 2118-2120.
32. Martins, J.N., et al., *Electrical and rheological percolation in poly(vinylidene fluoride)/multi-walled carbon nanotube nanocomposites.* Polymer International, 2010. **60**(3): p. 430-435.
33. Z.-M. Dang, L.W., Y. Yin, Q. Zhang, Q.-Q. Lei,, *Giant Dielectric Permittivities in Functionalized Carbon-Nanotube/ Electroactive-Polymer Nanocomposites.* Advanced Materials, 2007. **19**(6): p. 852-857.
34. Li, Q., et al., *Large dielectric constant of the chemically functionalized carbon nanotube/polymer composites.* Composites Science and Technology, 2008. **68**(10-11): p. 2290-2296.
35. Connor, M.T., et al., *Broadband ac conductivity of conductor-polymer composites.* Physical Review B, 1998. **57**(4): p. 2286.
36. Silva, J., et al., *Applying complex network theory to the understanding of high aspect ratio carbon filled composites.* Europhysics Letters (EPL), 2011. **93**: p. 37005.
37. Li, Q., et al., *Temperature dependence of the electrical properties of the carbon nanotube/polymer composites.* Express Polymer Letters, 2009. **3**(12):

p. 769-777.
38. O'Bryan, G., et al., *Nanotube Surface Functionalization Effects in Blended Multiwalled Carbon Nanotube/PVDF Composites.* Journal of Applied Polymer Science, 2010. **120**(3): p. 1379-1384.
39. Chang, C.M. and Y.L. Liu, *Functionalization of multi-walled carbon nanotubes with non-reactive polymers through an ozone-mediated process for the preparation of a wide range of high performance polymer/carbon nanotube composites.* Carbon, 2010. **48**(4): p. 1289-1297.
40. Gonçalves, A.G., et al., *Influence of the surface chemistry of multi-walled carbon nanotubes on their activity as ozonation catalysts.* Carbon, 2010. **48**(15): p. 4369-4381.
41. Carabineiro, S.A., et al., *Effect of the carbon nanotube surface characteristics on the conductivity and dielectric constant of carbon nanotube/poly(vinylidene fluoride) composites.* Nanoscale Research Letters, 2011. **6**: p. 302 (5 pages).
42. Costa, P., et al., *The effect of fibre concentration on the [alpha] to [beta]-phase transformation, degree of crystallinity and electrical properties of vapour grown carbon nanofibre/poly(vinylidene fluoride) composites.* Carbon, 2009. **47**(11): p. 2590-2599.
43. Sencadas, V., R. Gregorio, and S. Lanceros-Méndez, *α to β Phase Transformation and Microestructural Changes of PVDF Films Induced by Uniaxial Stretch.* Journal of Macromolecular Science, Part B: Physics, 2009. **48**(3): p. 514 - 525.
44. Figueiredo, J.L., et al., *Modification of the surface chemistry of activated carbons.* Carbon, 1999. **37**(9): p. 1379-1389.
45. Figueiredo, J.L., et al., *Characterization of active sites on carbon catalysts.* Industrial & Engineering Chemistry Research, 2007. **46**(12): p. 4110-4115.
46. Banerjee, S., T. Hemraj-Benny, and S. Wong, *Covalent Surface Chemistry of Single-Walled Carbon Nanotubes.* Advanced Materials, 2005. **17**(1): p. 17-29.
47. Monthioux, M., et al., *Sensitivity of single-wall carbon nanotubes to chemical processing: an electron microscopy investigation.* Carbon, 2001. **39**(8): p. 1251-1272.
48. Lopes, A.C., et al., *Nucleation of the electroactive γ phase and enhancement of the optical transparency in low filler content poly(vinylidene)/clay nanocomposites.* Journal of Physical Chemistry C, 2011. **115**(37): p. 18076-18082.
49. Lanceros-Méndez, S., et al., *FTIR and DSC studies of mechanically deformed β-PVDF films.* Journal of Macromolecular Science - Physics, 2001. **40 B**(3-4): p. 517-527.
50. Kobayashi, M., K. Tashiro, and H. Tadokoro, *Molecular Vibrations of Three Crystal Forms of Poly(vinylidene fluoride).* Macromolecules, 1975. **8**(2): p. 158-171.
51. Salimi, A. and A.A. Yousefi, *Conformational changes and phase transformation mechanisms in PVDF solution-cast films.* Journal of Polymer Science Part B: Polymer Physics, 2004. **42**(18): p. 3487-3495.
52. Baskaran, N., *Conductivity relaxation and ion transport processes in glassy electrolytes.* Journal of Applied Physics, 2002. **92**(2): p. 825-833.
53. Sreenivasan, S., et al., *Effect of disorder strength on optimal paths in complex networks.* Physical Review E, 2004. **70**(4): p. 046133.
54. Ambegaokar, V., B.I. Halperin, and J.S. Langer, *Hopping Conductivity in Disordered Systems.* Physical Review B, 1971. **4**(8): p. 2612.